# Influence of the 4-Substituted Pyridine Ligand L′ on both the Conformation and Spectroscopic Properties of the (2,2′-Biquinoline-$\kappa N^1$,$\kappa N^{1'}$)tricarbonyl(pyridine-$\kappa N^1$)rhenium(1+) Complex ([$Re(CO)_3$(bqui)(py)]$^+$) and Its Derivatives [$Re(CO)_3(L)(L')]^+$ (L = 2,2′-Biquinoline and 3,3′-(Ethane-1,2-diyl)-2,2′-biquinoline)

by **Sergio A. Moya***[a]), **Juan Guerrero**[a]), **Felipe J. Rodriguez-Nieto**[b]), **Ezequiel Wolcan**[b]), **Mario R. Féliz**[b]), **Ricardo F. Baggio**[c]) , and **María T. Garland**[d])

[a]) Departamento de Química de los Materiales, Facultad de Química y Biología, Universidad de Santiago de Chile, Casilla 40-33, Santiago, Chile (fax: 56-2-6812108; e-mail: smoya@lauca.usach.cl or jguerrer@lauca.usach.cl)

[b]) Instituto de Investigaciones Fisicoquímicas Teóricas y Aplicadas (INIFTA; *CONICET-CICBA-UNLP*), Departamento de Química, Facultad de Ciencias Exactas, Universidad Nacional de La Plata, Casilla de Correo 16 Suc. 4, La Plata (1900), Argentina (fax 54-21-254642; e-mail: mfeliz@isis.unlp.edu.ar)

[c]) Universidad de Argentina, Departamento de Física (Lab. TANDAR), Comisión Nacional de Energía Atómica, Av. del Libertador 8250, 1429 Buenos Aires, Argentina (fax: 54-1-754-7121; e-mail: baggio@cnea.gov.ar)

[d]) Departamento de Física, Facultad de Ciencias Físicas y Matemáticas, Universidad de Chile, Santiago de Chile, Chile

A series of new rhenium(I) complexes of the type $[Re^I(CO)_3(L)(L')]^{n+}$ (L = 2,2′-biquinoline (bqui) or 3,3′-(ethane-1,2-diyl)-2,2′-biquinoline ($CH_2CN_2$)bqui); L′ = $CF_3SO_3^-$, pyridine (py), or 4-substituted pyridine (HOpy, Bzpy, or NCpy); $n = 0$ or 1) were prepared and characterized by FT-IR, $^1$H-NMR, UV/VIS and emission spectroscopy, luminescence lifetimes, and cyclic voltammetry. The pseudo-octahedral facial configuration was established by X-ray single-crystal diffraction analysis of two complexes and by a FT-IR study of all complexes. The [$Re(CO)_3$(bqui)(Bzpy)]($CF_3SO_3$) complex crystallizes in the form of two mirror isomers arising from the conformational mobility of the biquinoline ligand. A correlation between the metal-to-ligand charge-transfer (MLCT) emission maxima and the $\sigma^+$ *Hammett* parameter was established for the complexes of the bqui series, while such correlation was not observed for the complexes of the ($CH_2CH_2$)bqui series. No correlation between oxidation potentials and the *Hammett* parameters was established. The results were rationalized in function of the effect of the 4-substituted pyridine ligand on the octahedral distortion and conformational characteristic of the complexes. The $^1$H-NMR data confirmed these results.

**Introduction.** – Luminescent transition-metal complexes have been utilized as photosensitizers in areas such as solar-energy conversion, electron-transfer studies, chemiluminescent and electroluminescent systems, binding dynamics of heterogeneous media, and probes of macromolecular structure [1]. In this regard, much attention has been paid to $Re^I$ complexes in recent years [2]. Many of these compounds exhibit a wide variety of energetically accessible metal-to-ligand charge transfer (MLCT), ligand-to-ligand charge transfer (LLCT), and intraligand (IL) excited states [3].

Their chemical, photochemical, and photocatalytic properties have made rhenium(I) complexes with polypyridine ligands potential thermal, photochemical, and electrochemical catalyzers [1a][4]. Examples of these include the electroreduction

and photoreduction of $CO_2$ which could be of interest in the conversion and storage of solar energy [5].

The photophysical properties of the metal complexes are determined predominantly by the lowest-energy excited states [6]. However, the population of higher excited states leads to photochemical pathways. Thus, the control or modulation of the absorption and/or emission energy is a very important tool for the modification of the catalytic behavior of these complexes.

To evaluate the effect of structural modifications in the polypyridine ligand on the properties of the ground and excited states of these complexes, we have studied complexes of the general structure $[ReBr(CO)_3(L)]$ with L = bidentate polypyridine ligand [3h][7]. In previous studies of $[ReBr(CO)_3(R,R'bqui)]$, with R,R′bqui = 3,3′-R,R′-2,2′-biquinoline and R = R′ = H or Me, or R–R′ = $CH_2CH_2$ or $CH_2CH_2CH_2$, we found that the extended conjugation in the 2,2′-biquinoline (= bqui) ligand, as compared to 2,2′-bipyridine (bpy) ligand, causes a shift towards lower energy both in the MLCT band and in the reduction potential of the polypyridine ligand [7b,d]. Moreover, the conformational characteristic of the complexes caused by the distortion degree from the planarity in the bqui ligand induces a slight variation of these energies [7d]. We have associated the emissions in these complexes with parallel relaxation processes from an IL and a MLCT state [7e].

The substitution of the Br-ligand in the complexes $[ReBr(CO)_3(R,R'bqui)]$ by 4-substituted pyridine ligands (L′) containing electron-donating or electron-attracting groups represents a viable alternative to obtain both a new MLCT electronic state, *i.e.*, Re → pyridine, and inductive effects upon the energy of the Re → bqui MLCT [6][7e]. The objective of the present work is to rationalize the inductive effect of the 4-substituted pyridine ligand on the properties of biquinolinerhenium complexes. For this purpose, we report here the synthesis and spectroscopic studies of a new series of complexes of the type $[Re^I(CO)_3(L)(L')]^{n+}$, with L = 2,2′-biquinoline (bqui[1]) or 3,3′-(ethane-1,2-diyl)-2,2′-biquinoline ($(CH_2CH_2)$bqui[1]); L′ = $CF_3SO_3^-$, pyridine (py), or 4-substituted pyridines Xpy, *i.e.*, HOpy, Bzpy (Bz = benzyl), or NCpy, and $n = 0$ or 1.

**Results and Discussion.** – The prepared complexes $[Re^I(CO)_3(L)(L')]^{n+}$ are stable in air either as solids or in solution. They are soluble in several solvents of medium polarity. The conductivity values are in accordance with the formulae of the corresponding complexes.

The IR spectrum for the $[Re(CO)_3(L)(CF_3SO_3)]$ complexes (L = bqui or $(CH_2CH_2)$-bqui) show three strong bands in the carbonyl stretching region that arise from a facial configuration with a local $C_s$ symmetry of the carbonyl groups around a hexacoordinated Re-center. In case of complexes $[Re(CO)_3(L)(L')]$ with L′ = 4-substituted pyridine ligand = Xpy, the IR spectra exhibit two intense bands in the carbonyl stretching region. This behavior results from a $C_{3v}$ local symmetry for the CO groups in a facial configuration. The lowest-energy band is very broad, which can be attributed to a

---

[1]) Formerly, the following abbreviations were used instead of bqui and $(CH_2CH_2)$bqui; 2,2′-biquinoline = 0,2N and 3,3′-dimethylene-2,2′-biquinoline = 3,3′-(ethane-1,2-diyl)-2,2′-biquinoline = 2,2N, respectively. For systematic names, see *Exper. Part.*

decrease of the octahedral symmetry in the complexes with 4-substituted pyridine ligands [8].

Crystal structures were obtained by X-ray single-crystal diffraction analysis for $[Re(CO)_3(bqui)(py)](CF_3SO_3)$ and $[Re(CO)_3(bqui)(Bzpy)](CF_3SO_3)$ (*Table 1*). The compounds are mononuclear, with $[Re(CO)_3(bqui)(py)](CF_3SO_3)$ exhibiting just one molecule in the asymmetric unit while two mirror isomers, hereafter represented by *A* and *B*, are observed in the case of $[Re(CO)_3(bqui)(Bzpy)](CF_3SO_3)$. In both structures, the complex cations are electrically balanced by the triflate counteranions thus giving rise to neutral entities (*Fig. 1*). In both species, the Re environment conforms to a slightly distorted octahedron built up through the coordination of three carbonyl groups, the bidentate bqui ligand, and the py or Bzpy ligand. The N(3) atom of the pyridine ligand and the C(1) atom of one of the carbonyl units occupy the apical sites, and the basal plane is defined by C(2) and C(3) (of the remaining carbonyl groups) and N(1) and N(2) of the bqui ligand (arbitrary atom numbering, see *Fig. 1*). In all cases, the metal atom is slightly displaced from the mean plane along the apical line toward the py or Bzpy ligand (by 0.109(1)Å in $[Re(CO)_3(bqui)(py)](CF_3SO_3)$ and by 0.114(1) and 0.108(1)Å in *A* and *B*, resp., of $[Re(CO)_3(bqui)(Bzpy)](CF_3SO_3)$), suggesting a base with the aspect of a depressed square pyramid. The apical axes are rather linear (N(3)–Re(1)–C(1) 179.2(3)° in $[Re(CO)_3(bqui)(py)](CF_3SO_3)$, and 178.0(5) and 179.3(5)° in *A* and *B*, resp., of $[Re(CO)_3(bqui)(Bzpy)](CF_3SO_3)$) with small departures from the mean plane normals (4.3(2)° in $[Re(CO)_3(bqui)(py)](CF_3SO_3)$, and 6.3(3) and 5.3(2)° in *A* and *B*, resp., of bqui $[Re(CO)_3(bqui)(Bzpy)](CF_3SO_3)$). The Re–carbonyl interactions appear to be quite linear in $[Re(CO)_3(bqui)(py)](CF_3SO_3)$ (range of the O–C–Re angle, 177.4–179.5°) and show a slightly larger deviation in $[Re(CO)_3$-

Table 1. *Crystallographic Data*

| | $[Re(CO)_3(bqui)(py)](CF_3SO_3)$ | $[Re(CO)_3(bqui)(Bzpy)](CF_3SO_3)$ |
|---|---|---|
| Formula | $C_{27}H_{17}F_3N_3O_6ReS$ | $C_{34}H_{23}F_3N_3O_6ReS$ |
| $M_r$ | 754.70 | 844.81 |
| System | monoclinic | monoclinic |
| Space group | *P* 21/*c* (no.14) | *P* 21/*c* (no.14) |
| Crystal dimensions [mm] | 0.30×0.24×0.16 | 0.25×0.18×0.16 |
| Crystal color, shape | orange, prisms | orange, prisms |
| *a* [Å] | 11.614(1) | 23.670(5) |
| *b* [Å] | 12.597(1) | 10.755(2) |
| *c* [Å] | 18.234(2) | 27.235(7) |
| $\beta$ [°] | 98.31(1) | 111.84(2) |
| Cell volume [Å$^3$] | 2639.8(4) | 6436(2) |
| *Z* | 4 | 8 |
| $D_x$ [gcm$^{-3}$] | 1.90 | 1.74 |
| F(000) | 1464 | 3312 |
| $\mu$ [mm$^{-1}$] | 4.75 | 3.91 |
| Max, min absorpt. correct. | 0.39, 0.28 | 0.52, 0.43 |
| Unique refl., $R_{int}$, parameters | 4644, 0.051, 384 | 11317, 0.075, 880 |
| $R_1$[a]), $wR_2$[b]) ($F^2 > 2\sigma(F^2)$) | 0.044, 0.104 | 0.064, 0.119 |
| Final $\Delta\rho$ [eÅ$^{-3}$] | 1.76, −1.68 | 0.77, −0.87 |

[a]) $R_1$: $\Sigma\,||F_o|-|F_c||/\Sigma|F_o|$. [b]) $wR_2$: $[\Sigma[w(F_o^2-F_c^2)^2]/\Sigma[w(F_o^2)^2]]^{\frac{1}{2}}$.

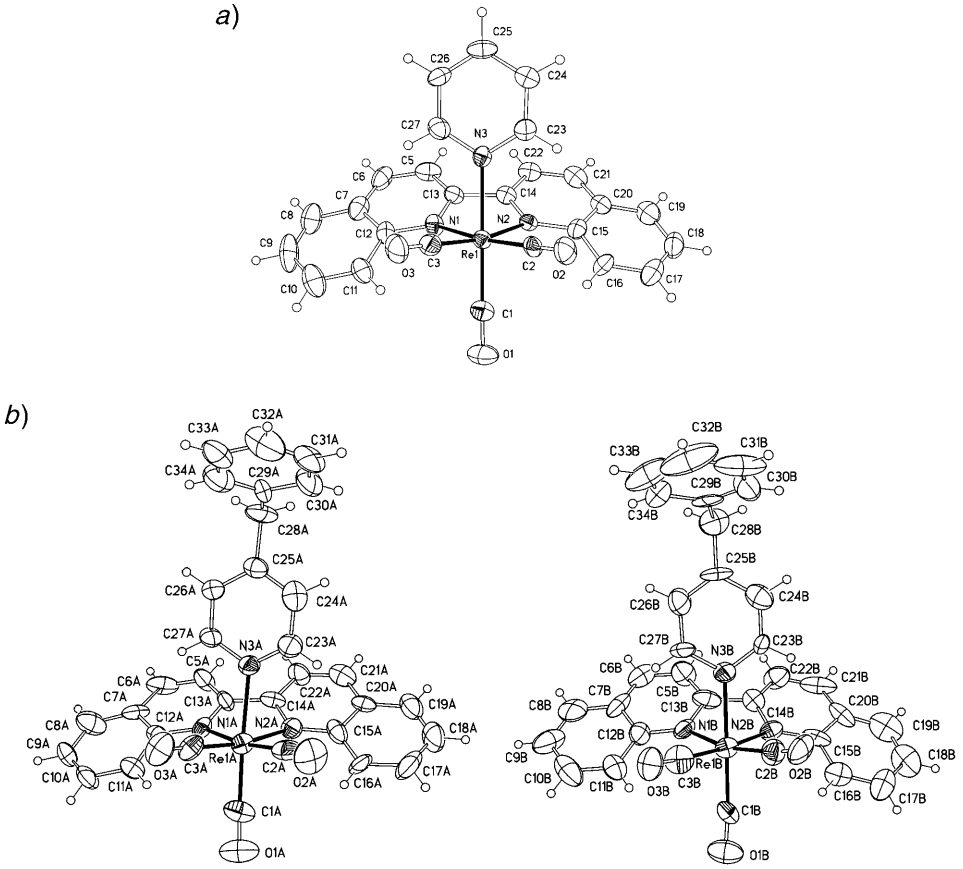


Fig. 1. *Molecular diagrams* a) *for* $[Re(CO)_3(bqui)(py)]^+$ *and* b) *for the isomers* A *and* B *of* $[Re(CO)_3(bqui)(Bzpy)]^+$. *Arbitrary atom numbering;* displacement ellipsoids drawn at a 40% level.

(bqui)(Bzpy)]($CF_3SO_3$) (ranges of the O–C–Re angle, 174.9–177.2° in *A* and 171.9–174.6° in *B*).

In the above complexes, the two independent moieties of the bqui ligand define a substantial dihedral angle (17.7° in [$Re(CO)_3$(bqui)(py)]($CF_3SO_3$), and 12.1° and 17.4° in *A* and *B*, resp., of [$Re(CO)_3$(bqui)(Bzpy)]($CF_3SO_3$)), much larger than the corresponding N(1)–C(13)–C(14)–N(2) torsion angle that would be a measure of any eventual rotation around the C(13)–C(14) bond (−4.6° in [$Re(CO)_3$(bqui)(py)]-($CF_3SO_3$) and 3.6° and −1.4° in *A* and *B*, resp., of [$Re(CO)_3$(bqui)(Bzpy)]($CF_3SO_3$)). This conformational effect probably is responsible for the presence of two conformational isomers.

This important deformation arises when the bqui ligand is bi-coordinate to the Re-center. The ligand is forced out of the octahedron's equatorial plane in the way discussed previously, presumably to avoid as much as possible the steric hindrance imposed by the eventual collision between the outermost H-atoms (H–C(8) and

H–C(8′)) of bqui and equatorial carbonyl groups (see below *Fig. 2* for bqui numbering). Due to the nonplanar character of the ligand, the effect is difficult to quantify properly. However, its importance is suggested by the rather large dihedral angles that the lateral wings subtend with the polyhedron equatorial plane N(1)–N(2)–C(2)–C(3) (arbitrary numbering, see *Fig. 1*). In complexes with the same coordination pattern but containing the smaller pyridine ligands, this angle usually amounts to only a few degrees; but this dihedral angle is 35.3 and 37.7° in $[Re(CO)_3(bqui)(py)](CF_3SO_3)$, and 32.9 and 35.1°, and 35.6 and 36.5° in *A* and *B*, respectively, of $[Re(CO)_3(bqui)(Bzpy)](CF_3SO_3)$. These observations reveal an additional effect on this angle caused by the L′ ligands. In all cases, the bqui ligand is tilted towards the py or Bzpy side of the coordination sphere.

The $^1$H-NMR spectra of the complexes are summarized in *Tables 2* and *3*. The assignments of the chemical shifts were made by comparison with data from previously reported studies of the free ligands and the precursor complexes [7d] [9]. Generally, the signals of the aromatic pyridine protons overlapped with those of the biquinoline protons. However, the characteristic *AB* pattern for the former protons are clearly distinguished in the spectra of the complexes with the Bzpy ligand.

The increase of deshielding of all the biquinoline protons observed in the new complexes relative to the precursor complexes with a Br-ligand, notably of H–C(4,4′) localized in the *p*-position of the coordinated N-atom, is a good indication that the pyridine ligands induce a lower electron density on the Re-atom as compared to the Br and triflate ligands. Similarly, an effect of the 4-substituted pyridine ligand Xpy on the $\delta$(H) of the aromatic biquinoline protons is observed in both complex series (*Tables 2* and *3*).

The two *m* signals of the $CH_2CH_2$ protons of the $(CH_2CH_2)$bqui ligand in the $[Re(CO)_3\{(CH_2CH_2)bqui\}(CF_3SO_3)]$ complex is characteristic for an $A_2B_2$ system (*Table 3* and *Fig. 2*). This pattern is due to the presence, in solution, of two conformers in slow exchange. Both mirror-image isomers are generated by the distortion of the $(CH_2CH_2)$bqui ligand in the complexes (*Fig. 1*, *b*). This $A_2B_2$ pattern is also observed for the $[ReBr(CO)_3\{(CH_2CH_2)bqui\}]$ precursor complex [7b,d], but the chemical-shift difference between the $H_a$ and $H_b$ protons decreases in the $[Re(CO)_3\{(CH_2CH_2)bqui\}(Xpy)]^+$ complexes. As shown in *Table 3*, these differences could be as small as those observed for the $[Re(CO)_3\{(CH_2CH_2)bqui\}(py)]^+$ complex for which the $A_2B_2$ signals collapse to a quasi-*s* (*Fig. 2*, *b* and *c*). This behavior is expected for isomers in a fast exchange motion. The change in the shift difference between the $H_a$ and $H_b$ signals along the L′ series of complexes indicates that the conformational-motion rate depends on the pyridine ligands at the working temperature.

The UV/VIS data of the complexes $[Re(CO)_3(L)(CF_3SO_3)]$ (*Table 4*) reveal one solvent-polarity-dependent band around 430 nm that has been assigned to a rhenium-to-biquinoline (Re → bqui) charge-transfer (MLCT) transition [3c] [7b,d]; for the $[Re(CO)_3(L)(Xpy)]^+$ complexes, this band can be clearly observed as one or two shoulders of low intensity above 400 nm. In the $[Re(CO)_3(L)(Xpy)]^+$ complexes, these MLCT transitions are shifted to higher energies than those found in the complexes with Br or triflate ligands, in agreement with a lower electron density on the metal center induced by the pyridine ligand. However, it is not possible to evaluate the inductive effect of the Xpy ligand on the MLCT band due to partial overlap with the intraligand-transition bands ($\pi \rightarrow \pi^*$ biquinoline). The expected band below

Table 2. *$^1$H-NMR Data of the [Re(CO)$_3$(bqui)(L′)]$^{n+}$ ($n=0$ or 1) Complexes and of the Free bqui Ligand*[a])

| | bqui | | | | | | L′[b]) | | |
|---|---|---|---|---|---|---|---|---|---|
| | H–C(3,3′) | H–C(4,4′) | H–C(6,6′) | H–C(8,8′) | H–C(5,5′) | H–C(7,7′) | $H_\alpha$ | $H_\beta$ | $H_x$ |
| bqui | 8.85 (*d*) | 8.30 (*d*) | 7.58 (*t*) | 8.25 (*d*) | 7.86 (*d*) | 7.75 (*t*) | | | |
| [ReBr(CO)$_3$(bqui)] | 8.31 (*d*) | 8.50 (*d*) | 7.71 (*t*) | 8.96 (*d*) | 7.94 (*m*) | 7.94 (*m*) | | | |
| [Re(CO)$_3$(bqui)(CF$_3$SO$_3$)] | 8.39 (*d*) | 8.67 (*d*) | 7.83 (*m*) | 8.92 (*d*) | 8.03 (*m*) | 8.03 (*m*) | | | |
| $\Delta\delta$[c]) | −0.46 | +0.37 | +0.25 | +0.67 | +0.17 | +0.28 | | | |
| [Re(CO)$_3$(bqui)(HOpy)]$^+$ | 8.35 (*d*) | 8.52 (*d*) | 7.70 (*dt*) | 8.95 (*d*) | 7.90 (*m*) | 7.90 (*m*) | 7.70 (*d*) | 5.99 (*d*) | 2.65 (*s*)[d]) |
| $\Delta\delta$[c]) | −0.50 | +0.22 | +0.12 | +0.70 | +0.04 | +0.15 | | | |
| [Re(CO)$_3$(bqui)(Bzpy)]$^+$ | 8.82 (*d*) | 8.84 (*d*) | 7.86 (*dt*) | 8.84 (*d*) | 8.12 (*d*) | 8.09 (*dt*) | 6.95 (*d*) | 6.72 (*d*) | 3.83 (*s*)[e]) |
| $\Delta\delta$[c]) | −0.03 | +0.54 | +0.28 | +0.59 | +0.26 | +0.34 | | | 7.16 (*m*)[f]) |
| | | | | | | | | | 6.97 (*td*)[f]) |
| | | | | | | | | | 7.16 (*m*)[f]) |
| [Re(CO)$_3$(bqui)(NCpy)]$^+$ | 8.48 (*d*) | 8.80 (*d*) | 7.72 (*t*) | 8.92 (*d*) | 8.10 (*d*) | 7.91 (*dt*) | 8.20 (*d*) | 7.70 (*d*) | |
| $\Delta\delta$[c]) | −0.37 | +0.50 | +0.14 | +0.67 | +0.24 | +0.16 | | | |
| [Re(CO)$_3$(bqui)(py)]$^+$ | 8.70 (*AB*) | 8.70 (*AB*) | 7.70 (*t*) | 8.91 (*d*) | 8.00 (*m*) | 8.00 (*m*) | 8.00 (*m*) | 8.00 (*m*) | 7.10 (*dt*) |
| $\Delta\delta$[c]) | −0.15 | +0.40 | +0.12 | +0.66 | +0.14 | +0.25 | | | |

[a]) $\delta$ in ppm rel. to internal $SiMe_4$ at 25° in $CDCl_3$. [b]) For convenience, the H-atoms in *o*- and *m*-position to the N-atom of all pyridine ligands L′ are indicated by $H_\alpha$ and $H_\beta$, respectively. [c]) $\Delta\delta=\delta_{complex}-\delta_{bqui}$. [d]) $H_x$ = O*H* of 4-hydroxypyridine. [e]) $H_x$ = C$H_2$ of 4-benzylpyridine, [f]) $H_x$ = 5 arom. H of Ph.

Table 3. *$^1$H-NMR Data of the [Re(CO)$_3${(CH$_2$CH$_2$)bqui}(L′)]$^{n+}$ (n = 0 or 1) Complexes and of the Free (CH$_2$CH$_2$)bqui Ligand*[a])

| | (CH$_2$CH$_2$)bqui[b]) | | | | | | L′[c]) | | | |
|---|---|---|---|---|---|---|---|---|---|---|
| | H–C(4,4′) | H–C(6,6′) | H–C(8,8′) | H–(5,5′) | H–C(7,7′) | H$_a$ | H$_b$ | H$_\alpha$ | H$_\beta$ | H$_x$ |
| (CH$_2$CH$_2$)bqui | 8.03 (*s*) | 7.52 (*t*) | 8.43 (*d*) | 7.77 (*d*) | 7.68 (*t*) | 3.20 (*s*) | | | | |
| [ReBr(CO)$_3${(CH$_2$CH$_2$)qbqui}] | 8.21 (*s*) | 7.66 (*t*) | 8.84 (*d*) | 7.86 (*m*) | 7.86 (*m*) | 3.35 ($A_2B_2$) | 3.26 ($A_2B_2$) | | | |
| [Re(CO)$_3${(CH$_2$CH$_2$)bqui}(CF$_3$SO$_3$)] | 8.38 (*s*) | 7.74 (*t*) | 8.82 (*d*) | 7.97 (*m*) | 7.97 (*m*) | 3.32 ($A_2B_2$) | 3.54 ($A_2B_2$) | | | |
| $\Delta\delta$[d]) | +0.35 | +0.22 | +0.39 | +0.20 | +0.29 | | | | | |
| [Re(CO)$_3${(CH$_2$CH$_2$)bqui}(HOpy)]$^+$ | 8.35 (*s*) | 7.70 (*dt*) | 8.84 (*d*) | 8.30 (*d*) | 7.91 (*t*) | 3.38 ($A_2B_2$) | 3.42 ($A_2B_2$) | 7.91 | 7.89 (*AB*) | 2.35 (*s*)[e]) |
| $\Delta\delta$[d]) | +0.32 | +0.18 | +0.41 | +0.53 | +0.23 | | | | | |
| [Re(CO)$_3${(CH$_2$CH$_2$)bqui}(Bzpy)]$^+$ | 8.59 (*s*) | 7.80 (*i*) | 8.72 (*d*) | 8.09 (*dd*) | 8.00 (*dt*) | 3.13 ($A_2B_2$) | 3.18 ($A_2B_2$) | 7.0 7(*d*) | 6.83 (*d*) | 3.82 (*s*)[f]) |
| $\Delta\delta$[d]) | +0.56 | +0.28 | +0.29 | +0.32 | +0.32 | | | 6.96 (*dd*)[g]) | 7.14 (*d*)[g]) | 7.14 (*m*)[g]) |
| [Re(CO)$_3${(CH$_2$CH$_2$)bqui)}(NCpy)]$^+$ | 8.37 (*s*) | 7.85 (*t*) | 8.76 (*d*) | 8.43 (*d*) | 7.90 (*t*) | 3.30 ($A_2B_2$) | 3.50 ($A_2B_2$) | 7.95 (br.) | 7.80 (*d*) | |
| $\Delta\delta$[d]) | +0.34 | +0.33 | +0.33 | +0.66 | +0.22 | | | | | |
| [Re(CO)$_3${(CH$_2$CH$_2$)bqui)}(py)]$^+$ | 8.62 (*s*) | 7.88 (*m*) | 8.76 (*d*) | 8.20 (*d*) | 8.00 (*dt*) | 3.26 (*s*) | 3.26 (*s*) | 7.88 (*m*) | 7.21 (*m*) | 7.21 (*m*) |
| $\Delta\delta$[d]) | +0.59 | +0.36 | +0.33 | +0.43 | +0.32 | | | | | |

[a]) $\delta$ in ppm rel. to internal SiMe$_4$ at 25° in CDCl$_3$. [b]) For convenience, the ligand (CH$_2$CH$_2$)bqui is numbered like bqui (see *Fig. 2*); H$_a$ and H$_b$ are the atoms of the CH$_2$CH$_2$ link. [c]) For convenience, the H-atoms in *o*- and *m*-position to the N-atom of all pyridine ligands L′ are indicated by H$_\alpha$ and H$_\beta$, respectively. [d]) $\Delta\delta = \delta_{complex} - \delta_{(CH_2CH_2)bqui}$. [e]) H$_x$ = O*H* of 4-hydroxypyridine. [f]) H$_x$ = C*H*$_2$ of 4-benzylpyridine. [g]) H$_x$ = 5 arom. H of Ph.

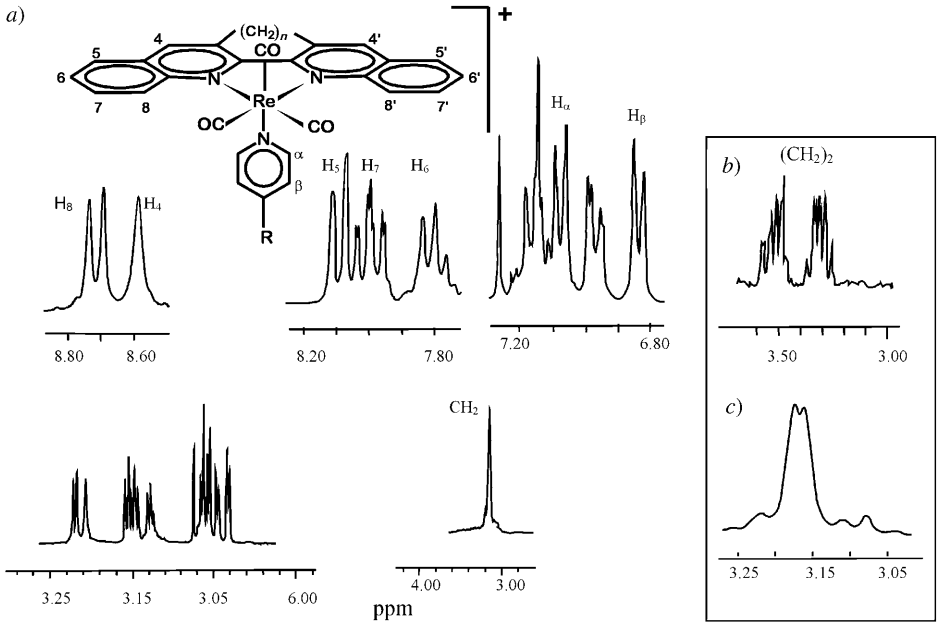


Fig. 2. a) *$^1$H-NMR Spectrum of [Re(CO)$_3${(CH$_2$CH$_2$)bqui}(Bzpy)]$^+$*, b) *CH$_2$CH$_2$ $^1$H-NMR signals of the ReBr(CO)$_3$[(CH$_2$CH$_2$)bqui]] precursor, and* c) *CH$_2$CH$_2$ $^1$H-NMR signals of [Re(CO)$_3${(CH$_2$CH$_2$)-bqui}(Bzpy)]$^+$*. $CDCl_3$ solutions at room temperature; for atom numbering see formula and *Footnotes b* and *c* in *Table 3*.

400 nm for the Re-to-Xpy charge-transfer excited state [10][7d] was not observed because it is overlapped by more intense bands corresponding to L intraligand transitions.

*Fig. 3,a* shows the emission spectra for the bqui and ($CH_2CH_2$)bqui ligands and for the corresponding perchlorate salts, *i.e.*, bqui·2 $HClO_4$ and ($CH_2CH_2$)bqui·2 $HClO_4$, when these compounds are excited with $\lambda_{exc}$ 250 nm in MeCN. The inset in *Fig. 3,a* illustrates the protonation effect upon the UV/VIS spectra of bqui and ($CH_2CH_2$)bqui. It is observed that both the absorption and emission maxima of ($CH_2CH_2$)bqui experience a shift to lower energies after protonation. The emission spectrum of bqui experiences minor changes towards lower energies after protonation; for bqui, the first excited singlet state is of n$\pi^*$ character, and its lowest triplet state is assigned as $\pi\pi^*$ [7i]. Inspection to *Fig. 3,a* suggests that, after protonation of ($CH_2CH_2$)bqui, fluorescence from the $^1n\pi^*$ state ($\lambda_{em}$ *ca.* 360 nm) diminishes, as expected, and the phosphorescence from the $^3\pi\pi^*$ state ($\lambda_{em}$ *ca.* 430 nm) is increased, for the unprotonated ($CH_2CH_2$)bqui ligand, there is a mixture of fluorescence and phosphorescence. Besides that, the emission quantum yield $\phi_{em}$ increases by a factor of 5 after the protonation of ($CH_2CH_2$)bqui. The bqui and ($CH_2CH_2$)bqui·2 $HClO_4$ compounds, however, show mainly fluorescence with a lower contribution from the $^3\pi\pi^*$ state to the total luminescence. Luminescence quantum yields for bqui and bqui·2 $HClO_4$ are nearly the same. The emission quantum yield $\phi_{em}$ for ($CH_2CH_2$)bqui·2 $HClO_4$, after excitation with $\lambda_{exc}$ 250 nm, is nearly 10-fold higher than that of bqui·2 $HClO_4$. This can be explained by the hindrance to rotation

Table 4. *UV/VIS Data for Rhenium(I) Complexes at 25°*

| Compound | Solvent | $\lambda_{abs}$ [nm] ($10^{-3}$ $\varepsilon$/dm$^3$ mol$^{-1}$ cm$^{-1}$) | | |
|---|---|---|---|---|
| | | ($t_{2g} \rightarrow \pi^*_L$) | | ($\pi \rightarrow \pi^*$) |
| $[Re(CO)_3(bqui)(CF_3SO_3)]$ | $CH_2Cl_2$ | 440 (1.5) | 374 (8.1) | 356 (5.2) |
| | $Me_2O$ | 430 (sh) | 373 (17.1) | 265 (69.3) |
| | MeCN | 424 (3.6) | 371 (12.4) | 354 (20.3) |
| $[Re(CO)_3(bqui)(HOpy)]^+$ | $CH_2Cl_2$ | 430 (6.0) | 374 (296.0) | 262 (567.3) |
| | $Me_2O$ | 420 (sh) | 373 (285.5) | 357 (200.7) |
| | MeCN | 420 (sh) | 372 (254.4) | 350 (sh) |
| $[Re(CO)_3(bqui)(NCpy)]^+$ | $CH_2Cl_2$ | 425 (sh) | 376 (234.0) | 264 (411.9) |
| | $Me_2O$ | 420 (sh) | 374 (262.2) | 357 (226.4) |
| | MeCN | 418 (sh) | 379 (sh) | 373 (366.0) |
| $[Re(CO)_3(bqui)(py)]^+$ | $CH_2Cl_2$ | 420 (sh) | 374 (295.9) | 262 (567.3) |
| | $Me_2O$ | 414 (sh) | 373 (285.5) | 357 (200.7) |
| | MeCN | 405 (sh) | 372 (254.4) | 267 (568.6) |
| $[Re(CO)_3(bqui)(Bzpy)]^+$ | $CH_2Cl_2$ | 416 (sh) | 379 (304.0) | 362 (208.0) |
| | EtOH | 410 (sh) | 378 (279.3) | 361 (197.2) |
| | MeCN | 400 (sh) | 377 (280.2) | 268 (532.0) |
| $[Re(CO)_3\{(CH_2CH_2)bqui\}(CF_3SO_3)]$ | $CH_2Cl_2$ | 450 (sh) | 395 (5.5) | 271 (17.7) |
| | EtOH | 430 (sh) | 394 (3.1) | 266 (9.1) |
| | MeCN | 426 (0.4) | 371 (12.4) | 354 (2.0) |
| $[Re(CO)_3\{(CH_2CH_2)bqui\}(HOpy)]^+$ | $CH_2Cl_2$ | 450 (sh) | 394 (251.1) | 378 (209.8) |
| | EtOH | 438 (sh) | 394 (165.1) | 378 (143.1) |
| | MeCN | 430 (sh) | 392 (250.5) | 268 (584.0) |
| $[Re(CO)_3\{(CH_2CH)bqui\}(NCpy)]^+$ | $CH_2Cl_2$ | 451 (sh) | 395 (199.3) | 379 (168.0) |
| | EtOH | 435 (sh) | 393 (187.7) | 377 (223.9) |
| | MeCN | 425 (sh) | 395 (254.8) | 268 (473.3) |
| $[Re(CO)_3\{(CH_2CH_2)bqui\}(py)]^+$ | $CH_2Cl_2$ | 445 (sh) | 340 (250.0) | |
| | EtOH | 430 (sh) | 392 (81.6) | 268 (178.9) |
| | MeCN | 420 (sh) | 391 (169.9) | 267 (348.0) |
| $[Re(CO)_3\{(CH_2CH_2)bqui\}(Bzpy)]^+$ | $CH_2Cl_2$ | 451 (sh) | 400 (350.6) | 268 (533.1) |
| | EtOH | 445 (sh) | 399 (215.1) | 269 (410.5) |
| | MeCN | 435 (sh) | 395 218.6) | 269 (502.7) |

imposed by the $CH_2CH_2$ group in $(CH_2CH_2)$bqui as compared to the 'free' bqui which leads to a smaller nonradiative rate constant.

When solutions of the $Re^I$ complexes are optically excited with $\lambda_{ex}$ 250, 350, and 400 nm, three different emission spectra are obtained (*Fig. 3,b*) with $\lambda_{em}$ near 370, 420, and 650 nm, respectively. The emission properties of the $Re^I$ complexes are shown in *Table 5*. The emission with $\lambda_{em}$ near 370 nm (*Fig. 3,b*) exhibits some vibrational structure, and it was observed for all the complexes under study. Moreover, this emission is very similar to that obtained for bqui, $(CH_2CH_2)$bqui, and bqui·2 $HClO_4$ (see *Fig. 3,a*). The emission with $\lambda_{em}$ near 370 nm could, therefore, be attributed to the fluorescence arising from the bqui moiety. The emission with $\lambda_{em}$ near 650 nm which shifts to the red (*Fig. 4*) when the solvent polarity is increased, corresponds to a MLCT (Re → bqui) excited state [7e].

To analyze the effect of the 4-substituted pyridine ligands on the HOMO of the $Re^I$ complex, the emission maxima ($1/\lambda_{em}$) were plotted against the $\sigma^+$ *Hammett* parameters. Emission and absorption energies augment with an increase in the electron-withdraw-

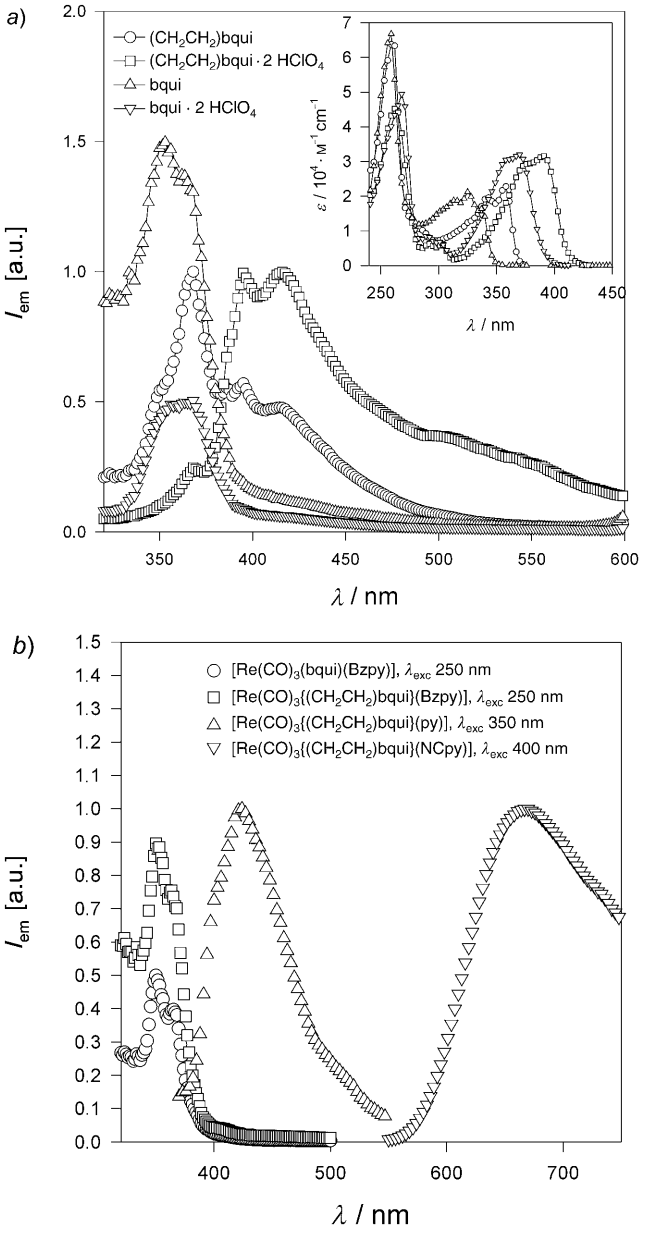


Fig. 3. a) *Room-temperature emission spectra of the ligands bqui* (△) *and (CH$_2$CH$_2$)bqui* (○) *and of the corresponding perchlorate salts bqui·2 HClO$_4$* (▽) *and (CH$_2$CH$_2$)bqui·2 HClO$_4$* (□) *after irradiation with* $\lambda_{exc}$ *250 nm* (the corresponding UV/VIS spectra are given in the inset). b) *Room-temperature emission spectra of [Re(CO)$_3$(bqui)(Bzpy)]$^+$* (○; $\lambda_{exc}$ 250 nm) *[Re(CO)$_3${(CH$_2$CH$_2$)bqui}(Bzpy)]$^+$* (□; $\lambda_{exc}$ 250 nm), *[Re(CO)$_3$(bqui)(py)]$^+$* (△; $\lambda_{exc}$ 350 nm) *and [Re(CO)$_3${(CH$_2$CH$_2$)bqui}(NCpy)]$^+$* (▽; $\lambda_{exc}$ 400 nm) *in MeCN at different excitation wavelengths.*

Table 5. *Photophysical Properties of the [Re(CO)$_3$(L)(L')]$^+$ Complexes and the L Ligands at Room Temperature*

| | L | L′ | Solvent | $\lambda_{exc}$ 250nm | $\lambda_{exc}$ 400 nm | | $\lambda_{exc}$ 350 nm | | $\tau_{em}$ [ns] | |
|---|---|---|---|---|---|---|---|---|---|---|
| | | | | $\Phi_{em}$ | $\lambda_{em}$ [nm] | $\Phi_{em}$ | $\lambda_{em}$ [nm] | $\Phi_{em}$ | $\lambda_{exc}$ 355 nm | $\lambda_{exc}$ 337 nm |
| [Re(CO$_3$(L)L′)]$^+$ | bqui | HOpy | MeCN | $(3.0\pm1)\cdot10^{-3}$ | 692 | $(3.8\pm0.4)\cdot10^{-4}$ | 416 | $(1.0\pm0.1)\cdot10^{-5}$ | | |
| | bqui | Bzpy | MeCN | $(5.6\pm0.8)\cdot10^{-3}$ | 686 | $(2.0\pm0.2)\cdot10^{-3}$ | 404 | $(1.4\pm0.1)\cdot10^{-5}$ | | 36[b]) |
| | bqui | py | MeCN | $(1.9\pm0.4)\cdot10^{-3}$ | 675 | $(2.3\pm0.2)\cdot10^{-3}$ | 404 | $(1.7\pm0.2)\cdot10^{-5}$ | | 40[b]) |
| | bqui | NCpy | $C_6H_6$ | | 650 | | 404 | | 11, 141[a]) | |
| | | | $CH_2Cl_2$ | | 664 | | 470 | | 8, 73[a]) | |
| | | | $C_2H_5O$ | | 666 | | 404 | | | |
| | | | MeCN | $(3.0\pm1)\cdot10^{-3}$ | 671 | $(8.2\pm0.8)\cdot10^{-4}$ | 430 | $(3.2\pm0.1)\cdot10^{-5}$ | 8, 44[a]) | |
| | $(CH_2CH_2)$bqui | HOpy | MeCN | $(1.8\pm0.1)\cdot10^{-3}$ | 670 | $(6.7\pm0.7)\cdot10^{-5}$ | 401 | $(1.2\pm0.1)\cdot10^{-4}$ | | |
| | $(CH_2CH_2)$bqui | Bzpy | MeCN | $(2.0\pm0.4)\cdot10^{-3}$ | 686 | $(1.4\pm0.1)\cdot10^{-3}$ | 401 | $(4.6\pm0.5)\cdot10^{-5}$ | | 35[b]) |
| | $(CH_2CH_2)$bqui | py | MeCN | $(5.8\pm0.4)\cdot10^{-3}$ | 686 | $(1.8\pm0.2)\cdot10^{-3}$ | 424 | $(1.3\pm0.1)\cdot10^{-4}$ | 33[b]) | 35[b]) |
| | $(CH_2CH_2)$bqui | NCpy | MeCN/$CH_2Cl_2$ | $(4.0\pm0.6)\cdot10^{-3}$ | 669 | $(6.8\pm0.7)\cdot10^{-4}$ | 418 | $(4.3\pm0.4)\cdot10^{-4}$ | 16, 97[a]) | |
| | | | | | | | | | 11, 75[a]) | |
| | bqui | pz | MeOH/$CH_2Cl_2$ | – | – | – | – | – | 4, 113[c]) | |
| | | | MeCN | – | | | | | 6, 114[c]) | |
| | bqui | 4,4′bpy | MeOH/$CH_2Cl_2$ | – | – | – | – | – | 5, 58[c] | |
| Free ligands | | | | | | | | | | |
| | bqui | | MeCN | $(4.0\pm0.4)\cdot10^{-3}$ | | | | | | |
| | bqui·2 $HClO_4$ | | MeCN | $(3.6\pm0.4)\cdot10^{-3}$ | | | | | | |
| | $(CH_2CH_2)$bqui | | MeCN | $(6.9\pm0.7)\cdot10^{-3}$ | | | | | | |
| | $(CH_2CH_2)$bqui·2 $HClO_4$ | | MeCN | $(3.2\pm0.3)\cdot10^{-2}$ | | | | | | |

[a]) Biexponential decay. [b]) Monoexponential decay. [c]) Taken from [3i]; pz = pyrazine, 4,4′bpy = 4,4′-bipyridine.

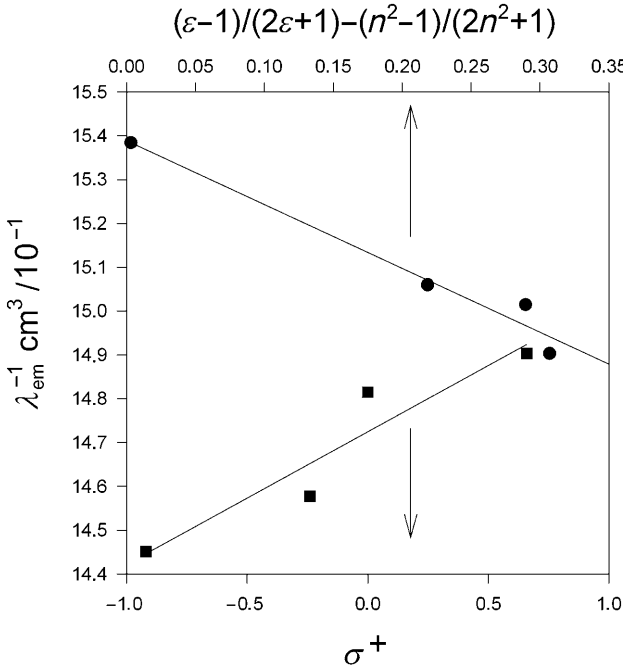


Fig. 4. Lippert *Plot for the dependence of the emission energy of [Re(CO)$_3$(bqui)(NCpy)]$^+$ on solvent polarity (*top of *x* axis*) and dependence of the emission energy of the bqui complexes on* Hammett *parameter* $\sigma^+$ (bottom of *x* axis). For $\sigma^+$ values, see *Exper. Part;* for details see *Table 6.*

ing power of the pyridine substituents, with more positive $\sigma^+$'s providing more electron-withdrawing power. It is known that $\sigma^+$ shows a better correlation with cationic species. The formation of a MLCT excited state (Re → bqui) makes the metal more positive ($Re^{II}$) with the resultant formation of positive charge on the pyridine ligand as the consequence of partial withdrawal of electron density from the metal. Therefore, ligands with more basic (more negative) $\sigma^+$ values, like $OH^-$ will drive electron density into the Re, making it more easily oxidized and lowering the MLCT energy; for the bqui series, a linear correlation is observed between $1/\lambda_{em}$ and $\sigma+$ (*Fig. 4*). However, the ($CH_2CH_2$)bqui series did not show a good correlation (*Table 5*). This lack of correlation in the ($CH_2CH_2$)bqui series could reflect the conformational effect of the pyridine ligand on the whole complex that may modify both the LUMO and HOMO energies [7d]. This conformational effect is better compensated in the series of the [Re(CO)$_3$(bqui)L′]$^+$ complexes than in that of the [Re(CO)$_3$\{($CH_2CH_2$)bqui\}L′]$^+$ complexes due to the major restriction of the conformational motion in this latter series.

Another emission, with $\lambda_{em}$ near 420 nm, is illustrated in *Fig. 3,b* for the [Re(CO)$_3$\{($CH_2CH_2$)bqui\}(py)]$^+$ complex but was observed for all the complexes of both the bqui and the ($CH_2CH_2$)bqui series after excitation with $\lambda_{exc}$ 350 nm (*Table 5*). This emission is strongly dependent on the solvent, but no correlation could be established between emission maxima and solvent polarity. However, the emission near 420 nm is similar to that of ($CH_2CH_2$)bqui·2 HCl in *Fig. 3,a*. It could be assigned

to the $^3\pi\pi^*$ ($^3$IL) excited states of the bqui and $(CH_2CH_2)$bqui ligands in the $Re^I$ complexes. It is noteworthy that the emission quantum yield $\phi_{em}$ ($\lambda_{exc}$ 350 nm) is higher by a factor of 10 for the complexes of the $(CH_2CH_2)$bqui series than for those of the bqui series (see the comment above concerning the difference of $\phi_m$ for $(CH_2CH_2)$bqui·2 $HClO_4$ and bqui·2 $HClO_4$)

After excitation with $\lambda_{exc}$ 400 nm (MLCT (Re → bqui) excited state) in both the bqui and $(CH_2CH_2)$bqui series, the lowest emission quantum yields $\phi_{em}$ are obtained for the complexes with the 4-substituted ligand HOpy, while the highest values are obtained for those with the py and Bzpy ligands (*Table 5*). After excitation with $\lambda_{exc}$ 350 nm, the $\phi_{em}$ are between two and ten-fold lower than the corresponding $\phi_{em}$ after excitation with $\lambda_{exc}$ 400 nm in both the bqui and $(CH_2CH_2)$bqui complex series. After excitation with $\lambda_{exc}$ 250 nm, the $\phi_{em}$ amount to $2-6\cdot10^{-3}$ for all the bqui and $(CH_2CH_2)$bqui complexes and are in general higher than the $\phi_{em}$ after excitation with $\lambda_{exc}$ 400 nm.

It is possible to account for the biexponential decay of the luminescence in the $[ReBr(CO)_3\{(CH_2CH_2CH_2)bqui\}]$ complex ($(CH_2CH_2CH_2)$bqui = 3,3′-(propane-1,3-diyl)-2,2′-biquinoline) by considering the parallel relaxations of the lowest lying $^3$MLCT and $^3$IL states [7e]. Moreover, $[Re(CO)_3(bqui)L]^+$ complexes with L = pyrazine (pz) and 4,4′-bipyridine (4,4′bpy) (see *Table 5*) showed a biexponential decay of the luminescence with a longer lifetime, $\tau_{em}$ 58 ns for L = 4,4′bpy and $\tau_{em}$ 114 ns for L = pz, assigned to the radiative and nonradiative relaxations of the $^3$MLCT (Re → bqui) excited state, and a shorter lifetime, $\tau_{em}$ *ca.* 6 ns, assigned to the decay of the $^3$IL states [3i]. In the present study (see *Table 5*), the luminescence lifetimes for the $Re^I$ complexes were obtained after a curve fitting analysis of the oscillographic traces, monitoring wavelengths between 400 and 650 nm. However, the longer lifetime was not observed at monitoring wavelengths between 400 and 500 (where there is no $^3$MLCT (Re → bqui) emission). Only monitoring wavelengths between 550 and 650 showed the longer luminescence lifetime. Therefore, it can be stated that the longer luminescence lifetimes (ranging from 33 to 141 ns in *Table 5*) for $[Re(CO)_3(bqui)(NCpy)]^+$, $[Re(CO)_3\{(CH_2Cl_2)bqui\}(NCpy)]^+$, $[Re(CO)_3\{(CH_2CH_2)bqui\}(py)]^+$, $[Re(CO)_3(bqui)(py)]^+$, $[Re(CO)_3\{(CH_2CH_2)bqui\}(Bzpy)]^+$, and $[Re(CO)_3(bqui)(Bzpy)]^+$ can be ascribed to the luminescence decay of the $^3$MLCT (Re → bqui) excited state. The weak luminescence of $[Re(CO)_3\{(CH_2CH_2)bqui\}(OHpy)]^+$ and $[Re(CO)_3(bqui)(OHpy)]^+$ did not allow us to measure emission lifetimes with $\lambda_{exc}$ 355 or 337 nm. The shorter lifetime, $\tau_{em}$ *ca.* 8–16 ns, which was mainly observed with monitoring wavelengths between 400 and 500 nm, must be ascribed to the $^3$IL state.

The excitation spectra in *Fig. 5*, which are normalized to the emission-quantum-yield values of *Table 5*, show that the highest $\phi_{em}$ are observed on irradiations at $\lambda_{ex}$ 420 nm when monitoring the emission at $\lambda_{em}$ 650 nm, and at $\lambda_{ex}$ 340 nm when the emission is monitored at $\lambda_{em}$ 420 nm. Nevertheless, the emission corresponding to the $^3$MLCT (Re → bqui) is still significant when the excitation energy is near $\lambda_{ex}$ 340 nm. Some contribution from the IL excited state to the emission with $\lambda_{em}$ near 650 nm can not be discarded when exciting with $\lambda_{ex}$ 350 nm since the biquinoline absorption spectrum is still significant at that wavelength. In *Fig. 5*, the UV/VIS spectrum of the $[Re(CO)_3\{(CH_2CH_2)bqui\}(NCpy)^+$ complex in MeCN is shown for comparison. The lowest absorption band for this complex is placed between the two peaks of the two

excitation spectra. It was established in a previous work [7e] that a short-lived $^3$IL state of the bqui ligand is placed between 15 and 20 kJ above the $^3$MLCT (Re → bqui) state. Intersystem crossing from the $^3$IL to the $^3$MLCT (Re → bqui) state has been proposed in [3i]. The shortening of the $^3$IL-state lifetime, $\tau_{em}$ *ca.* 8–16 ns, in both the bqui and $(CH_2CH_2)$bqui complex series can be compared to the longer lifetimes (*ca.* 900 ns) of the $^3$IL excited states in $[ReCl(CO)_3L_2]$ complexes (L = quinoline or isoquinoline) where the MLCT state is placed at higher energy than the $^3$IL excited state [7j]. The shortening of the the $^3$IL-state lifetime in the $[Re(CO)_3(bqui)(L')]^+$ and $[Re(CO)_3\{(CH_2CH_2)bqui\}(L')]^+$ complexes can be explained by a fast intersystem crossing, *i.e.*, on a time scale $\tau < 20$ ns, between $^3$IL and $^3$MLCT excited states.

Redox potentials of the rhenium complexes are shown in *Table 6*. The complexes may be divided into two groups based on their electrochemical properties. The first group involves the py and Bzpy derivatives of the bqui and $(CH_2CH_2)$bqui series and is characterized by two successive reversible reduction waves between 0.00 and −2.00 V (*vs.* SCE) and only one reversible oxidation wave between 0.00 and +2.00 V (*vs.* SCE). The second group includes the OHpy and NCpy derivatives of both series, where four reversible reduction waves are found between 0.00 and −2.00 V (*vs.* SCE) and one irreversible oxidation wave between 0.00 and +2.00 V (*vs.* SCE).

According to previous studies [7b,d], the first reduction wave of the first group could be attributed to a ligand-centered process that involves the addition of an electron to the $\pi^*$ orbital on the bqui moiety. Three possible processes could be assigned to the second reduction wave, *i*) a metal-centered $Re^I/Re^0$ reduction, *ii*) a pyridine-ligand reduction, and *iii*) a second reduction of the bqui moiety.

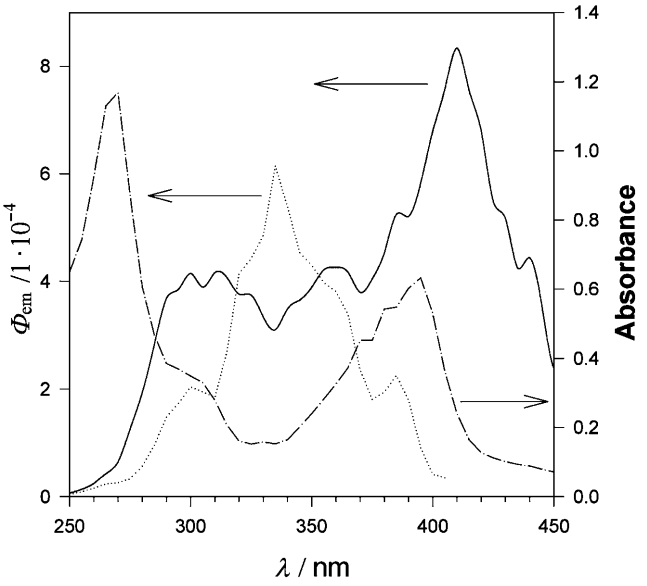


Fig. 5. *Excitation spectra of* $[Re(CO)_3\{(CH_2CH_2)bqui\}(NCpy)]^+$ *in MeCN monitored at the emission wavelength:* $\lambda_{em}$ *650 nm* (—) *and 420 nm* (…) *and absorption spectrum of* $[Re(CO)_3\{(CH_2CH_2)_2bqui\}(NCpy)]^+$ (– · – · –) *in MeCN*

Table 6. *Electrochemical Data of the Complexes*[a])

| | Redox potential | | |
|---|---|---|---|
| | $E_{red}$/V | | $E_{ox}$/V |
| $[Re(CO)_3(bqui)(HOpy)]^+$ | −0.79, −0.89 | −1.38, −1.57 | +1.54[b]) |
| $[Re(CO)_3(bqui)(Bzpy)]^+$ | −0.71 | −1.24 | +1.71 |
| $[Re(CO)_3(bqui)(py)]^+$ | −0.71 | −1.24 | +1.72 |
| $[Re(CO)_3(bqui)(NPpy)]^+$ | −0.71, −0.90 | −1.26, −1.47 | +1.41[b]) |
| $[Re(CO)_3(bqui)(HOpy)]^+$ | −0.75, −0.90 | −1.29, −1.40 | +1.55[b]) |
| $[Re(CO)_3\{(CH_2CH_2)bqui\}(Pzpy)]^+$ | −0.71 | −1.25 | +1.70 |
| $[Re(CO)_3\{(CH_2CH_2)bqui\}(Py)]^+$ | −0.71 | −1.24 | +1.72 |
| $[Re(CO)_3\{(CH_2CH_2)bqui\}(NCpy)]^+$ | −0.77, −0.90 | −1.23, −1.49 | +1.56[b]) |

[a]) The experimental error in the potential measurements is ±0.01 V. [b]) Irreversible wave.

The change in the pyridine-ligand basicity should affect the complex mainly by destabilizing the $e_g$ orbitals. The lack of such an effect of the substituent at the pyridine ligand on the second reduction potential values eliminates process *i*) as a possible explanation. Process *ii*) may also be discarded considering that the reduction values are the same for both the Bzpy and py complexes. Therefore, a second reduction of the bqui moiety must be involved in the second reduction wave. Moreover, a difference of *ca.* 500 mV between the first and the second reduction potential is consistent with previous findings for similar complexes showing a similar electrochemical behavior [11].

For the second group, the appearance of four reversible waves might be explained by considering that the OHpy and NCpy ligands could generate a slow conformational motion between both enantiomers (established by X-ray and NMR). Consequently, two bqui moieties with different electrochemical behavior may be observed.

Each of the complexes displayed a reversible or irreversible oxidation between 1.00 and 2.00 V (*vs.* SCE) corresponding to a metal-centered process $Re^{I/II}$. This process involves the removal of an electron from the $t_{2g}$ orbitals of $Re^I$ [7d][12].

The effect of the basicity of the L′ ligand on the metal was analyzed considering the correlation between the oxidation potentials and the *Hammett* parameter. The lack of this correlation can be rationalized taking three aspects into account: first, the complexes with the OHpy and NCpy ligands show irreversible oxidation waves; second, the $t_{2g}$ orbitals should be, by symmetry, less affected by altering the pyridine basicities rather than the $e_g$ ones; and finally, the substituent at the pyridine ligand provides a different influence on the planarity of the bqui moiety, which may affect sterically the $t_{2g}$ energy. In accordance with the previous discussion, the importance of the latter effect is notable and has been also observed in related complexes [7d][13].

**Conclusion.** – X-Rays studies of rhenium and manganese complexes containing the same bqui and $(CH_2CH_2)$bqui ligands have revealed that the symmetry of the compounds is departing by various degrees from a perfect octahedron [7d,g,h][13b]. This deviation has a significant influence on the spectroscopic and electrochemical properties of the complexes [7]. Changes in the electronic repulsion between the d orbital of the metal and the bqui orbitals as the consequence of biquinoline conformational dis-

tortions are responsible for these influences. Destabilization of the LUMO and stabilization of the HOMO will usually result from an increase of this conformational distortion.

The bqui complexes with L′ ligands show different correlations with the *Hammett* parameter. The lack of a similar correlation for the corresponding ($CH_2CH_2$)bqui complexes reveals an additional influence of the L′ ligand on both the conformational- and exchange-motion rate of the complexes. This influence can presumably not be evaluated. However, it constitutes a promising alternative to modulate the complex properties.

We thank *DICYT-Usach*, *FONDECYT-Chile* (Projects 1050168 and 29500074-95), *CONICET-Argentina*, and *CICBA-Argentina* for financial support. Emission spectra were taken at INIBIOLP. The authors wish to thank Dr. *H. Garda* for his assistance.

## Experimental Part

*General*. The values of $\sigma^+$ in the *Lippert* plot (*Fig. 4*) are taken from [17]. All the operations were carried out under purified $N_2$ by standard *Schlenk* and vacuum-line techniques and by using freshly distilled, dried, and degassed solvents. The solvents used in preparations, crystallizations, and spectroscopic analysis (*Mallinckrodt*, grade HPLC) were distilled prior to use. For electrochemical studies, anh. MeCN was dried over $CaH_2$ under $N_2$ by refluxing for 2 h and then freshly distilled prior to use. Commercially available (*Aldrich*) 2,2′-biquinoline (bqui)[1]) and pyridine ligands, $AgCF_3SO_3$, [$ReBr(CO)_5$], and precursor compounds were used without further purification. The synthesis of the 3,3′-(ethane-1,2-diyl)-2,2′-biquinoline ligand (=6,7-dihydrodibenzo[*b*,*j*][1,10]-phenanthroline; ($CH_2CH_2$)bqui[1]) [9] and precursor complexes [$ReBr(CO)_3$(L)] have been previously described [7b,d]. Molar conductivities: *Cole-Parmer-01481* conductivity meter; $10^{-3}$M solns., in MeCN at 25°. UV/VIS Spectra: *Shimadzu-UV-160* spectrophotometer; quartz cells; solns. in purified solvents of different polarity at r.t. IR Spectra: *Bruker-IFS-66-V* FT-IR spectrophotometer; solid KBr disks; KBr cell (0.2 mm); scanned at least 100 times; in $cm^{-1}$. $^1$H-NMR Spectra: *250-MHz-Bruker* spectrometer. Microanalyses were performed at the Facultad de Química y Farmacia, Universidad de Chile.

*X-Ray Crystal-Structure Analyses.* The X-ray single-crystal diffraction data were collected in a *Siemens-R3m* four-circle diffractometer, with the $\omega/2\theta$ scan mode and a variable scan speed of 4.2–29.3° $min^{-1}$. Structures were solved by direct methods [14] and refined by full-matrix least squares in $F^2$ [15]. Anisotropic displacement factors were used for non-H-atoms, while H-atoms (all of which were unambiguously defined by the configuration) were included at their idealized positions and allowed to consider their presence onto their host atoms. A check for higher symmetry present in [$Re(CO)_3$(bqui)(Bzpy)]($CF_3SO_3$) was unsuccessful. The results are given in *Table 1* and *Fig. 1* (see [16] for the drawn displacement ellipsoids). CCDC-169685 and -169686 contains the supplementary crystallographic data for this paper. This data can be obtained free of charge from the *Cambridge Crystallographic Data Center via* www.ccdc.can.ac.uk/data_request/cif.

*Cyclic Voltammetry.* The measurements were performed by standard techniques [7d]. A sweep rate of 200 mV $s^{-1}$ was used for all the scans. Potentials are reported as $E_{\frac{1}{2}}=\frac{1}{2}(E_{p_a}+E_{p_c})$, where $E_{p_a}$ and $E_{p_c}$ are the anodic and cathodic peak potentials, respectively.

*Photophysical Measurements.* The luminescence of the $Re^I$ complexes at r.t. was investigated with an *SLM-Aminco-4800* or a *Perkin-Elmer-LS-50B* spectrofluorimeter connected to a PC. The spectra were corrected for differences in instrumental response and light scattering. Solns. were deoxygenated by bubbling $N_2$ of high purity in a gas-tight apparatus before recording the spectra. Emission quantum yields were measured relative to rhodamine B in EtOH. Quantum yields were calculated according to *Eqn. 1*, where *I* is the integral of the emission spectrum, *A* is the absorbance of the sample or standard at the excitation wavelength, and *n* is the solvent refraction index. Luminescence lifetime measurements were performed by excitation with the third harmonic of a *Spectron-Nd-YAG* laser (18 ns FWHM and 12 mJ/pulse at 355 nm) or with a *Laseroptics* nitrogen laser (7 ns FWHM and 2mJ/pulse at 337 nm).

$$\phi_{em}=(A_{standard}/A_{sample})(I_{sample}/I_{standard})\phi_{em,standard}(n_{sample}/n_{standard})^2 \quad (1)$$

*Synthesis of Rhenium Complexes.* The $[Re(CO)_3(L)(CF_3SO_3)]$ complexes [13b] were obtained by reaction of the $[ReBr(CO_3)(L)]$ complex with silver trifluoromethanesulfonate in $CH_2Cl_2$ at 50° during 4 h, under an inert atmosphere. AgBr was separated by passing the mixture through *Celite*. The filtrate was evaporated and the obtained solid purified by column chromatography (alumina, $CH_2Cl_2$). The eluate was evaporated, and pure crystals were isolated after crystallization.

The $[Re(CO)_3(L)(L')](CF_3SO_3)$ complexes [13b] were obtained at 50° under an inert atmosphere by addition of the corresponding 4-substituted pyridine in stoichiometric amounts to the $[Re(CO)_3(L)(CF_3SO_3)]$ complex dissolved in $CH_2Cl_2$. After 2 h, The resulting orange soln. was evaporated and the solid product purified by column chromatography (alumina, $CH_2Cl_2$/MeOH 95:5) The eluate was evaporated and a microcrystalline orange product was obtained after dropwise addition of cool hexane. All the complexes were characterized by elemental analysis, IR, molar conductivities, and melting points.

*(2,2′-Biquinoline-κN$^{1}$,κN$^{1'}$)tricarbonyl(trifluoromethanesulfonato-κO)rhenium* ($[Re(CO)_3(bqui)(CF_3SO_3)]$: Yield 84%. Molar conductivity: 21 $Scm^2mol^{-1}$. M.p. 333° (dec.). IR 2029v*s*, 1935v*s*, 1914v*s*. Anal. calc. for $C_{22}H_{12}F_3N_2O_6ReS$: C 39.11, H 1.79, N 4.15; found: C 39.71, H 1.84, N 4.32.

*(2,2′-Biquinoline-κN$^{1}$,κN$^{1'}$)tricarbonyl(pyridin-4-ol-κN$^{1}$)rhenium(1+) Trifluoromethanesulfonate* ($[Re(CO)_3(bqui)(HOpy)](CF_3SO_3)$): Yield 79%. Molar conductivity: 110 S $cm^2$ $mol^{-1}$. M.p. 154° (dec.). IR: 2015v*s*, 1901v*s*. Anal. calc. for $C_{27}H_{17}F_3N_3O_7ReS$: C 42.08, H 2.22, N 5.45; found: C 41.74, H 2.40, N 5.65.

*(2,2′-Biquinoline-κN$^{1}$,κN$^{1'}$)tricarbonyl[4-(phenylmethyl)pyridine-κN$^{1}$]rhenium(1+) Trifluoromethanesulfonate* ($[Re(CO)_3(bqui)(Bzpy)](CF_3SO_3)$): Yield 83%. Molar conductivity: 130 $Scm^2mol^{-1}$. M.p. 213° (dec.). IR: 2030v*s*, 1922v*s*. Anal. calc. for $C_{34}H_{23}F_3N_3O_6ReS$: C 48.34, H 2.74, N, 4.97; found: C 48.13, H 2.76, N 5.15.

*(2,2′-Biquinoline-κN$^{1}$,κN$^{1'}$)tricarbonyl(pyridine-κN$^{1}$)rhenium(1+) Trifluoromethanesulfonate* ($[Re(CO)_3(bqui)(py)](CF_3SO_3)$): Yield 30%. Molar conductivity: 105 $Scm^2mol^{-1}$. M.p. 213° (dec.). IR: 2015v*s*, 1898v*s*. Anal. calc. for $C_{27}H_{17}F_3N_3O_6ReS$: C 42.97, H 2.27, N 5.57; found: C 43.24, H 2.33, N 5.81.

*(2,2′-Biquinoline-κN$^{1}$,κN$^{1'}$)tricarbonyl(pyridine-4-carbonitrile-κN$^{1}$)rhenium(1+) Trifluoromethanesulfonate* ($[Re(CO)_3(bqui)(NCpy)](CF_3SO_3)$): Yield 23%. Molar conductivity: 99 $Scm^2mol^{-1}$. M.p. 103° (dec.). IR: 2020v*s*, 1904v*s*. Anal. calc. for $C_{28}H_{16}F_3N_4O_6ReS$: C 43.13, H 2.07, N 7.19; found: C 43.49, H 2.26, N 7.47.

*Tricarbonyl(6,7-dihydrodibenzo[*b,j*][1,10]phenanthroline-κN$^{13}$,κN$^{14}$)(trifluoromethanesulfonato-κO)rhenium* ($[Re(CO)_3\{(CH_2CH_2)bqui\}](CF_3SO_3)$): Yield 87%. Molar conductivity: 18 $Scm^2mol^{-1}$. M.p. 347° (dec.). IR: 2031v*s*, 1927v*s*, 1903v*s*. Anal. calc. for $C_{24}H_{14}F_3N_2O_6ReS$: C 41.09, H 2.01, N 3.99; found: C 41.41, H 2.31, N 4.15.

*Tricarbonyl(6,7-dihydrodibenzo[*b,j*][1,10]phenanthroline-κN$^{13}$,κN$^{14}$)(pyridin-4-ol-κN$^{1}$)rhenium(1+) Trifluoromethanesulfonate* $[Re(CO)_3\{(CH_2CH_2)bqui\}(HOpy)](CF_3SO_3)$): Yield 63%. Molar conductivity: 109 $Scm^2mol^{-1}$. M.p. 141° (dec.). IR: 2020v*s*, 1897v*s*. Anal. calc. for $C_{29}H_{19}F_3N_3O_7ReS$: C 43.72, H 2.40, N 5.27; found: C 44.08, H 2.51, N 5.01.

*Tricarbonyl(6,7-dihydrodibenzo[*b,j*][1,10]phenanthroline-κN$^{13}$,κN$^{14}$)[4-(phenylmethyl)pyridine-κN$^{1}$)rhenium(1+) Trifluoromethanesulfonate* ($[Re(CO)_3\{(CH_2CH_2)bqui\}(Bzpy)](CF_3SO_3)$): Yield 83%. Molar conductivity: 120 $Scm^2mol^{-1}$(MeCN). M.p. 115° (dec.). IR: 2029v*s*, 1911v*s*. Anal. calc. for $C_{36}H_{25}F_3N_3O_6ReS$: C 49.65, H 2.89, N 4.83; found: C 48.80, H 2.78, N 5.04.

*Tricarbonyl(6,7-dihydrodibenzo[*b,j*][1,10]phenanthroline-κN$^{13}$,κN$^{14}$)(pyridine-κN$^{1}$)rhenium(1+) Trifluoromethanesulfonate* $[Re(CO)_3\{(CH_2CH_2)bqui\}(py)](CF_3SO_3)$: Yield 22%. Molar conductivity: 100 $Scm^2mol^{-1}$. M.p. 365° (dec.). IR: 2016v*s*, 1898v*s*. Anal. calc. for $C_{29}H_{19}F_3N_3O_6ReS$: C 44.61, H 2.45, N 5.38; found: C 44.65, H 2.26, N 5.52.

*Tricarbonyl(6,7-dihydrodibenzo[*b,j*][1,10]phenanthroline-κN$^{13}$,κN$^{14}$)(pyridine-4-carbonitrile-κN$^{1}$)rhenium(1+) Trilfuoromethanesulfonate* ($[Re(CO)_3\{(CH_2CH_2)bqui\}(NCpy)](CF_3SO_3)$): Yield 66%. Molar conductivity: 123 $Scm^2mol^{-1}$. M.p. 144° (dec.). IR: 2024v*s*, 1899v*s*. Anal. calc. for $C_{30}H_{18}F_3N_4O_6ReS$: C 44.72, H 2.25, N 6.95; found: C 45.01, H 2.57, N 6.55.

## REFERENCES

[1] a) 'Energy Resources Through Photochemistry and Catalysis', Ed. M. Grätzel, Academic Press, New York, 1983; b) K. Kalyanasundaram, *Coord. Chem. Rev.* **1982**, *46*, 159; c) F. E. Lytle, D. M. Hercules, *Photochem. Photobiol.* **1971**, *13*, 123; d) D. A. Buttry, F. A. Anson, *J. Am. Chem. Soc.* **1982**, *104*, 4824; e) H. S. White, A. J. Bard, *J. Am. Chem. Soc.* **1982**, *104*, 6891; f) F. Bolleta, V. Balzani, *J. Am. Chem. Soc.* **1982**, *104*, 4250; g) A. Vogler, L. El-Sayed, R. G. Jones, J. Namnath, A. W. Adamson, *Inorg. Chim. Acta* **1981**, *53*, L35; h) H. Kunkely, A. Merz, A. Vogler, *J. Am. Chem. Soc.* **1983**, *105*, 7241; i) K. Kalyanasundaram, in 'Photochemistry in Microheterogeneous System', Academic Press, New York, 1987; j) C. V. Kumar, J. K. Barton, N. J.

Turro, *J. Am. Chem. Soc*. **1985**, *107*, 5518; k) J. K. Barton, E. Lolis, *J. Am. Chem. Soc*. **1985**, *107*, 708; l) J. K. Barton, A. T. Danishefsky, J. M. Goldberg, *J. Am. Chem. Soc*. **1984**, *106*, 2172; m) R. M. Carlos, M. G. Neumann, *J. Photochem. Photobiol. A: Chem*. **2000**, *131*, 67; n) S. Encinas, A. M. Barthram, M. D. Ward, F. Barigelleti, S. Campagna, *Chem. Commun*. **2001**, 277; o) J. Luo, K. B. Reddy, A. S. Salameh, J. F. Wishart, S. S. Isied, *Inorg. Chem.* **2000**, *39*, 2321.

[2] S. S. Sun, A. J. Leas, *Organometallics* **2001**, *20*, 2353; S. Berger, A. Klein, W. Kaim, *Inorg. Chem.* **1998**, *37*, 5664; S. V. Wallendael, D. P. Shaver, D. P. Rillema, B. J. Yoblinski, M. Stathis, T. F. Guarr, *Inorg. Chem.* **1990**, *29*, 1761; G. Ferraudi, N. Nurakami, G. Ruiz, E. Wolcan, M. R. Feliz, *Inorg. Chim. Acta* **1994**, *221*, 161; J. A. Baiano, D. L. Carson, G. M. Wolosh, D. E. DeJesus, C. F. Knowles, E. G. Szabo, W. R. Murphy Jr., *Inorg. Chem.* **1990**, *29*, 2327; V. W. W. Yam, Y. Yang, J. Zhang, B. W. K. Chu, N. Zhu, O*rganometallics* **2001**, *20*, 4911; O. Ishifani, K. Kanai, Y. Yamada, K. Sakamoto, *Chem. Commun*. **2001**, 1514; S. S. Sun, A. J. Leas, O*rganometallics* **2002**, *21*, 39; V. W. W. Yam, *Chem. Commun.* **2001**, 789; R. Argazzi, E. Bertolasi, C. Chiorboli, C. A. Bignozzi, M. K. Itokazu, N. Y. Murakami, *Inorg. Chem*. **2001**, *40*, 6885; T. Scheiring, J. Fiedler, W. Kaim, *Organometallics* **2001**, *20*, 1437; G. Ruiz, E. Wolcan, M. R. Feliz, *J. Photochem. Photobiol., A* **1996**, *101*, 119.

[3] a) L. Vallace, D. C. Jackman, D. P. Rillema, J. W. Merkert, *Inorg. Chem*. **1995**, *34*, 5210; b) R. M. Leasure, L. A. Sacksteder, C. Nesselrodt, G. A. Reitz, J. N. Demas, B. A. DeGraff, *Inorg. Chem*. **1991**, *3*, 3722; c) M. S. Wrighton, D. L. Morse, *J. Am. Chem. Soc*. **1974**, *96*, 998; d) P. L. Giordano, M. S. Wrighton, *J. Am. Chem. Soc*. **1979**, *101*, 2888; e) P. L. Giordano, M. S. Wrighton, *Inorg. Chem*. **1977**, *16*, 160; f) G. J. Storr, D. J. Stufkens, A. Oskan, *Inorg. Chem*. **1992**, *31*, 1318; g) K. S. Schanze, D. B. MacQueen, T. A. Perkins, L. A. Cabana, *Coord. Chem. Rev.* **1993**, *122*, 63; h) M. R. Féliz, G. J. Ferraudi, *J. Phys. Chem.* **1992**, *96*, 3059; i) J. Guerrero, O. E. Piro, E. Wolcan, M. R. Féliz, G. J. Ferraudi, S. A. Moya, *Organometallics* **2001**, *20*, 2842; j) R. Lopez, A. M. Leiva, F. Zuloaga, B. Loeb, E. Norambuena, K. M. Omberg, J. R. Schoonover, D. Striplin, M. Devenney, T. J. Meyer, *Inorg. Chem*. **1999**, *38*, 2924.

[4] J. R. Shoonover, G. F. Strouse, R. B. Dyer, W. D. Bates, P. Chen, T. J. Meyer, *Inorg. Chem*. **1996**, *35*, 273; K. Kalyanasundaram, in 'Photosensitization and Photocatalysis Using Organometallic Compounds', Ed. L. Grätzel, Kluwer Academic Publishers, The Netherlands, 1993; J. A. Treadway, B. Loeb, R. Lopez, P. Anderson, F. R. Keeneand, T. J. Meyer, *Inorg. Chem*. **1996**, *35*, 2242; B. D. Rossenaar, F. Hartl, D. J. Stufkens, *Inorg. Chem*. **1996**, *35*, 6194; F. R. Keene, B. P. Sullivan, in 'Mechanism of Electrochemical Reduction of Carbon Dioxide Catalyzed by Transition Metal Complexes', Elsevier, Amsterdam, 1993; C. A. Terraza, J. Guerrero, S. A. Moya, F. M. Rabagliati, R. Quijada, *Polym. Bull*. **1998**, *40*, 27; C. A. Terraza, J. Guerrero, S. A. Moya, F. M. Rabagliati, *Polym. Bull.* **1998**, *41*, 669.

[5] G. Ruiz, E. Wolcan, A. L. Capparelli, M. R. Feliz, *Photochem. Photobiol. A,* **1995**, *89*, 61; B. P. Sullivan, C. M. Bolinger, D. Conrad, W. Vining, T. J. Meyer, *J. Chem. Soc., Chem. Commun.* **1985**, 1414; J. Hawecker, J. M. Lehn, R. J. Ziessel, *J. Chem. Soc., Chem. Commun*. **1983**, 536; C. Pac, K. Ishii, S. Yanagida, *Chem. Lett*. **1989**, 765; D. H. Gibson, H. He, *Chem. Commun*. **2001**, 2082.

[6] M. R. Feliz, G. J. Ferraudi, H. J. Altmiller, *J. Phys. Chem*. **1992**, *96*, 257; C. Kutal, A. J. Corbin, G. J. Ferraudi, *Organometallics*, **1987**, *6*, 553; G. Ruiz, F. Rodriguez-Nieto, E. Wolcan, A. L. Capparelli, M. R. Féliz, *J. Photochem. Photobiol. A* **1997**, *107*, 47.

[7] a) S. A. Moya, R Pastene, R. Schmidt, J. Guerrero, R. Sariego, R. Sartori, *Bol. Soc. Chil. Quím*. **1992**, *37*, 43; b) R. Sartori, J. Guerrero, R. Pastene, R. Schmidt, R. Sariego, S. A. Moya, *Bol. Soc. Chil. Quím*. **1992**, *37*, 311; c) S. A. Moya, R. Pastene, R. Schmidt, J. Guerrero, R. Sartori, *Polyhedron* **1992**, *11*, 1665; d) S. A. Moya, J. Guerrero, R. Pastene, R. Schmidt, R. Sariego, R. Sartori, J. Sans-Aparicio, I. Fonseca, M. Martinez-Ripoll, *Inorg. Chem*. **1994**, *33*, 2341; e) G. Ferraudi, M. R. Feliz, E. Wolcan, Y. Hsu, S. A. Moya, J. Guerrero, *J. Phys. Chem.* **1995**, *99*, 4929; f) S. A. Moya, R. Pastene, A. J. Pardey, P. Baricelli, *Bol. Soc. Chil. Quím*. **1996**, *41*, 251; g) J. Guerrero, S. A. Moya, R. Baggio, M. T. Garland, *Acta Crystallogr. Sect. C* **1998**, *54*, 1592; h) J. Guerrero, S. A. Moya, M. T. Garland, R. Baggio, *Acta Crystallogr. Sect. C* **1999**, *55*, 932; i) R. H. Clarke, P. Mitra, K. Vinodgopal, *J. Chem. Phys.* **1982**, *77*, 5288; j) N. Murakami Iha, G. Ferraudi, *J. Chem. Soc., Dalton Trans.* **1994**, 2565.

[8] M. J. Bermejo, J. Y. Ruiz, X. Solans, J. Vinaixa, *Inorg. Chem*. **1988**, *27*, 4385.

[9] R. P. Thummel, F. Lefoulon, *J. Org. Chem*. **1985**, *50*, 666.

[10] J. C. Luong, L. Nadjo, M. S. Wrighton, *J. Am. Chem. Soc.* **1978**, *100*, 5790.

[11] R. Lin, Y. Fu, C. P. Brock, T. Guarr, *Inorg. Chem.* **1992**, *31*, 4336; M. K. De Armond, K. W. Hanck, D. W. Wertz, *Coord. Chem. Rev*. **1985**, *64*, 65; J. B. Cooper, D. B. MacQueen, J. D. Petersen, D. W. Wertz, *Inorg. Chem*. **1990**, *29*, 3701.

[12] L. A. World, R. Duesing, P. Cheng, L. Della-Ciana, T. J. Meyer, *J. Chem. Soc., Dalton Trans.* **1991**, 849; W. Yang, K. S. Schanze, *Inorg. Chem*. **1994**, *33*, 1354; S. A. Moya, R. Pastene, R. Sartori, P. Dixneuf, H. Le Bozec, *J. Braz. Chem. Soc*. **1995**, *6*, 29.

[13] a) L. A. Sacksteder, A. P. Zipp, E. A. Brown, J. Streich, J. N. Demas, B. A. De Graff, *Inorg. Chem*. **1990**, *29*, 4335; b) S. A. Moya, J. Guerrero, R. Pastene, I. Azocar-Guzman, A. J. Pardey, *Polyhedron* **2002**, *21*, 439; c) J. K. Hino, L. Della-Ciana, W. J. Dressick, B. P. Sullivan, *Inorg. Chem*. **1992**, *31*, 3701.

[14] G. M. Sheldrick, 'SHELXS97. Program for Structure Resolution', University of Göttingen, Germany, 1997.

[15] G. M. Sheldrick, 'SHELXL97. Program for Structure Refinement', University of Göttingen, Germany, 1997.

[16] G. M. Sheldrick, 'XP in SHELXTL-PC', Version 5.0, Siemens Analytical X-ray Instruments, Inc., Madison, Wisconsin, USA, 1994.

[17] J. C. Scaiano, 'Handbook of Organic Photochemistry', Vol. II, CRC Press,1989; H. Eyring, 'Physical Chemistry. An Advanced Treatise', Vol. VII, Academic Press, 1975.

*Received June 28, 2005*